International Journal of Pharmaceutics 682 (2025) 125963

Contents lists available at ScienceDirect

International Journal of Pharmaceutics

journal homepage: www.elsevier.com/locate/ijpharm

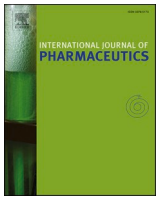

Hydrogel dressings loaded with anticancer/antimicrobial Ag(I) camphorimine complexes for treatment of malignant wounds

Joana P. Costa [a], Diana C. Silva [a,b], Fernanda Marques [c], Jeremias Muazeia [d], Jorge H. Leitão [d], Carlos A. Pinto [e], Jorge A. Saraiva [e], Ana P. Serro [a,b,*], M.Fernanda N.N. Carvalho [a,*]

[a] *Centro de Química Estrutural, Institute of Molecular Sciences and Departamento de Engenharia Química, Instituto Superior Técnico, Universidade de Lisboa, Avenida António José de Almeida, n° 12, 1000-043 Lisboa, Portugal*

[b] *Egas Moniz Center for Interdisciplinary Research, Egas Moniz School of Health & Science, 2829-511 Caparica, Almada, Portugal*

[c] *Centro de Ciências e Tecnologias Nucleares (C2TN) and Departamento de Engenharia e Ciências Nucleares, Instituto Superior Técnico, Universidade de Lisboa, Estrada Nacional 10 (km 139,7), 2695-066 Bobadela, Loures, Portugal*

[d] *iBB-Institute for Bioengineering and Biosciences, Associate Laboratory i4HB-Institute for Health and Bioeconomy at Instituto Superior Técnico, and Department of Bioengineering, Instituto Superior Técnico, Universidade de Lisboa, 1049-001 Lisbon, Portugal*

[e] *LAQV-REQUIMTE, Department of Chemistry, University of Aveiro, Campus Universitário de Santiago, 3810-193 Aveiro, Portugal*

A R T I C L E I N F O

Keywords:
Silver camphorimine complexes
HEMA hydrogel
Anticancer
Antibacterial
Wound dressings

A B S T R A C T

The treatment of skin wounds caused by metastatic lesions is often difficult because not many medicines exist that simultaneously act on cancer cells and bacteria. Such difficulty delays and sometimes compromises the treatment of oncologic patients. To contribute to face that problem a set of silver camphorimine compounds with antibacterial properties were assessed for activity against cancer cells A375 and MeWo melanoma cells using the MTT assay. From them, the silver camphorimine complex **1** displayed the highest combined anticancer and antibacterial activities and therefore was incorporated in a HEMA-based hydrogel to be used in a wound dressing. The hydrogel disks loaded with complex **1** effectively reduced suspensions of *E. coli, P. aeruginosa and B. contaminans* from the initial 5×10^5 CFU/mL to 0 CFU/mL after 24 and 48 h of incubation. In the case of *S. aureus*, a reduction of more than 99 % was observed after 24 h. However, after 48 h of incubation, the hydrogel was ineffective towards *S. aureus*. Although presenting a non-porous structure, the hydrogel revealed to be hydrophilic and able to retain a significant water content, allowing to keep the wound moist. Additionally, it exhibited mechanical and mucoadhesive properties suitable for treatments involving repeated and frequent dressing changes. The hydrogels were loaded with complex **1** by soaking and then sterilized by high hydrostatic pressure (HHP). Biocompatibility studies demonstrated that the loaded dressings were non-irritant and hemocompatible. The sterilization procedure did not affect the integrity of the complex, nor the drug release, which occurred in a sustained way through a non-Fickian diffusion mechanism. The dressing released 618.5 mg/cm^2/24 h, with nearly 90 % of the release occurring within the first 8 h. Considering the exudate production rates of chronic wounds and the MIC and MBC values for complex **1** it is expected that the dressings will be effective as antibacterial and anticancer agents. *In vivo* studies will be needed to confirm the clinical potential of the dressings. However, the produced dressings offer a promising approach for both infection control and cancer therapy in chronic wounds.

* Corresponding authors at: Centro de Química Estrutural, Institute of Molecular Sciences and Departamento de Engenharia Química, Instituto Superior Técnico, Universidade de Lisboa, Avenida António José de Almeida, n° 12, 1000-043 Lisboa, Portugal (M.F.N.N. Carvalho).

E-mail addresses: fmarujo@ctn.tecnico.ulisboa.pt (F. Marques), anapaula.serro@tecnico.ulisboa.pt (A.P. Serro), fcarvalho@tecnico.ulisboa.pt (M.FernandaN.N. Carvalho).

https://doi.org/10.1016/j.ijpharm.2025.125963
Received 14 March 2025; Received in revised form 24 June 2025; Accepted 10 July 2025
Available online 15 July 2025
0378-5173/© 2025 The Author(s). Published by Elsevier B.V. This is an open access article under the CC BY-NC-ND license (http://creativecommons.org/licenses/by-nc-nd/4.0/).

1. Introduction

Oncologic patients can develop wounds due to metastatic lesions that occur when cancer cells spread from primary tumors to the skin. During cancer treatment, these patients may be bedridden, with long periods in the same position that favor the formation of skin wounds or scars. Independently of their origin, these wounds are often painful, difficult to heal, and prone to infection, since these patients typically have depleted immune systems that facilitate the proliferation of opportunist bacteria and/or fungi. When infections involve resistant bacteria or fungi, the treatment options become limited, the recovery may then be delayed or even compromised, and the medical costs increase as well as the risk of mortality. Currently, the proliferation of antibiotićs resistant bacteria is one of the major concerns in global health. Among the antibiotic-resistant bacteria, *Pseudomonas aeruginosa* and *Staphylococcus aureus* were classified by the World Health Organization (WHO) (https://www.who.int/news-room/fact-sheets/detail/antimicrobial-resistance (2023)) as Priority Group (1) (Critical) and Priority Group (2) (High) concerning the need of efficient antibiotics. Several approaches are underway directed to the search for efficient antimicrobials to deal with resistant bacteria or fungi (e.g. *Candida auris*) (Shariq et al., 2023) One of them is based on the search for agents that fight microbial activity through mechanisms different from those of the antibiotics in use. (Rafique et al., 2010; Tran et al., 2013; Klebowski et al., 2018; Beyth et al., 2015; Frei, 2020a; Frei et al., 2020b; Crisan et al., 2021; Evans and Kavanagh, 2021) To date, a considerable number of new compounds with antimicrobial properties were identified but just a few fulfilled the requirements for therapeutic use. (https://reliefweb.int/report/world/antibacterial-agents-clinical-development-analysis-antibacterial-clinical-development. (accessed on 9 October 2023; Terreni et al., 2021) In what concerns oncologic patients, it would be desirable that the active principle that acts against the resistant microorganisms would also be effective against cancer cells. Under such purpose, coordination compounds may be favorable, since they can enhance antimicrobial activity by disrupting bacterial cell membranes, inhibiting enzymes, or interacting with bacterial DNA, which prevents the microorganism's replication and/or leads to their death. The metal ions in these compounds can also generate reactive oxygen species (ROS), leading to bacterial cells damage. (Sharma et al., 2022) Regarding cancer treatment, coordination compounds can interact with cancer cells DNA impairing their replication. They may also induce apoptosis by triggering cellular stress responses or inhibiting key enzymes involved in tumor cell survival. Additionally, the metal center can influence the compound's ability to target specific biomolecules in cancer cells, enhancing selectivity (Ndagi and Mhlongo, 2017). Although there are several anticancer agents based on coordination compounds (*e.g. cis*-platin), (Muhammad and Guo, 2014; Jungwirth et al., 2011; Lazarevi et al., 2017; Lucaciu et al., 2022) there is a growing demand for chemotherapy drugs. (Muhammad and Guo, 2014).

The treatment of complicated wounds, such as those mentioned above, involves the application of dressings that provide protection against external agents and allow exudate to be managed, maintaining a moist and balanced healing environment. An innovative approach to face wound infections in oncologic patients while fighting cancer is the use of hydrogel dressings that incorporate antimicrobial and anticancer coordination compounds. (Chifiriuc et al., 2022) Hydrogels for wound dressings may be prepared from different materials, namely biocompatible natural and synthetic polymers. The homo or co-polymers based on 2-hydroxyethylmethacrylate (HEMA) are among the most used materials in ophthalmic lenses, wound dressings (Radhakumary et al., 2011) and production of biomedical devices. HEMA-based materials demonstrate high biocompatibility, non-toxicity, good wetting and swelling ability. (Singh and Dhimanm, 2015) Their properties are often improved through the addition of other components such as hyaluronate, (Radhakumary et al., 2011) chitosan (Luo et al., 2023) poly (ethylene glycol), (Bayramoğlu et al., 2009) or poly vinylpyrrolidone (PVP). (Grytsenko et al., 2018) Grytsenko *et al* (Grytsenko, xxxx) produced HEMA/PVP materials with silver particles for dressings to be used in the treatment of venous ulcers. These materials showed antibacterial and antifungal activity against *S. aureus*; *S. epidermidis*; *Streptococcus viridans*, *E. coli* and *Candida albicans* due to the presence of silver in the hydrogel films. In another study, Tang *et al* (Tang et al., 2010) used a sequential formation technique to produce double network hydrogels of polyHEMA/PVP and then loaded them with a model drug (methylene blue) with known affinity for negative charged materials. The produced materials demonstrated good swelling capacity, relatively high oxygen permeability and drug loading capability, leading to a sustained drug release, which makes from the material a potential candidate to be used in wound dressings.

Within our work, several silver camphorimine complexes were identified as having antimicrobial (Leitão et al., 2018; Cardoso et al., 2017) and /or anticancer properties (in some cases with high selectivity). (Costa et al., 2022) Focused on the potential topical applications of these compounds as antibacterial agents for patients with skin cancer, the cytotoxicity of Ag(I) camphorimine complexes with antibacterial activity was assessed towards A375 and MeWo melanoma cells cancer cells. The complex that displayed the best combined antimicrobial /antimicrobial properties was selected to be incorporated into a HEMA/PVP hydrogel to produce a therapeutic dressing for cancer related wounds. The drug release behavior was evaluated, and the material was characterized regarding the most relevant properties for dressing application, namely water content, swelling ratio, mechanical properties, wettability, morphology, mucoadhesion, irritability and hemocompatibility.

2. Results and discussion

2.1. Antimicrobial and anticancer activity of the Ag(I) camphorimine complexes

The antimicrobial and/or anticancer activities of silver camphorimine compounds based on ligands of the types, ^{A}L ($OC_{10}H_{14}NY$), ^{B}L ($O_2SNC_{10}H_{13}NR$) and ^{C}L ($(OC_{10}H_{14}N)_2Z$) (Fig. 1) was accessed in previous studies showing their efficacy against mammalian cancer cells and/or Gram-negative and Gram-positive pathogenic agents. (Leitão et al., 2018; Cardoso et al., 2017) However, only a few displayed combined anticancer and antibacterial properties.

Aiming at incorporate Ag(I) camphorimine complexes in hydrogels and establish the conditions to prepare multifunctional dressings for the wound treatment of skin cancer patients, a selection of Ag(I) camphor complexes with former identified antimicrobial properties (Leitão et al., 2018) was studied. An exhaustive approach was used starting with the evaluation of the cytotoxic activity of silver camphorimine ([$Ag(NO_3)$(^{A1}L)], **1**; [$Ag(NO_3)(^{A2}L)_2$), **2**; [$Ag(NO_3)(^{A3}L)_2$), **3**; [$Ag(NO_3)(^{A4}L)_2$), **4**; [$Ag(OH)(^{A2}L)]\cdot H_2O$, **5**; [$Ag(OH)(^{B1}L)]\cdot CH_3COOH$, **6**; [$Ag(NO_3)(^{B2}L)_2]\cdot H_2O$, **7**; [$Ag(NO_3)(^{C1}L)$], **8**) compounds towards human melanoma A375 cells and MeWo cells. These cell lines have distinct characteristics. The A375 cells are known for their epithelial morphology, high tumorigenic potential and metastatic potential, while MeWo cells are known for their fibroblast-like morphology and a moderate tumorigenic and metastatic potential. (Lewandowski et al., 2022) The compounds were also assessed towards HDF and V79 fibroblasts to ascertain their toxicity against normal cells. Results are displayed in Table 1, together with data on their activity against different bacteria.

The IC_{50} values show that no matter the type of silver co-ligand (NO_3^-, OH^-) or the type of camphorimine ligand (^{A}L, ^{B}L or ^{C}L, Fig. 1), the complexes display considerable cytotoxic activity against A375 and MeWo cells upon a short exposure (24 h). Among the complexes, the bi-camphor complex **8** displays the lowest IC_{50} values (6.6 ± 1.6 μM and 9.0 ± 1.8 μM for A375 and MeWo, respectively) thus the highest cytotoxic activity. However, compound **8** displays the lowest antibacterial activity towards all the bacteria under study (*Escherichia coli*,

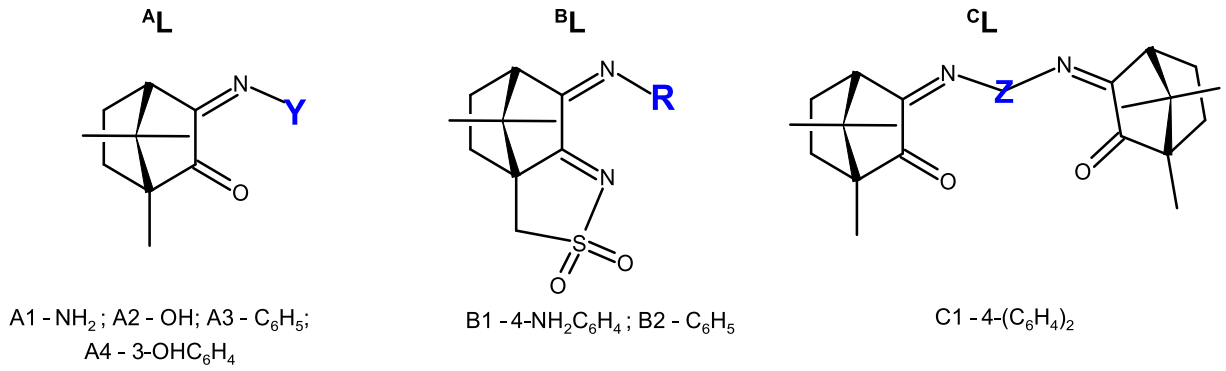

Fig. 1. Camphorimine type of ligands ^{A}L, ^{B}L and ^{C}L.

Table 1
Cytotoxic[a] and antibacterial[b] activities of silver camphorimine complexes and silver nitrate.

Complex	A375 IC_{50} (μM)[a]	MeWo	HDF	V79	SI[c]	MIC[b,d] (μg/mL)	
1[e]	11.0 ± 3.0	13.9 ± 2.1	18.7 ± 6.3	13.7 ± 3.0	1.7	*E. coli*	22
						P. aeruginosa	27
						B. contaminans	27
						S. aureus	56
2	17.7 ± 5.2	22.7 ± 4.1	22.7 ± 7.2	27.3 ± 7.6	1.3	*E. coli*	51
						P. aeruginosa	52
						B. contaminans	59
							119
						S. aureus	
3	11.6 ± 2.5	24.6 ± 5.0	18.1 ± 4.8	31.0 ± 8.2	1.6	*E. coli*	59
						P. aeruginosa	55
						B. contaminans	91
							54
						S. aureus	
4	14.8 ± 3.6	19.4 ± 5.0	17.4 ± 3.6	18.2 ± 5.1	1.2	*E. coli*	52
						P. aeruginosa	53
						B. contaminans	75
							113
						S. aureus	
5	22.1 ± 9.3	22.1 ± 9.3	35.3 ± 9.1	–	1.6	*E. coli*	7.2
						P. aeruginosa	3.4
						B. contaminans	6.4
							9.3
						S. aureus	
6	31.4 ± 8.7	31.4 ± 8.7	45.6 ± 10	31.8 ± 4.9	1.5	*E. coli*	15.6
						P. aeruginosa	11.2
						B. contaminans	16.1
						S. aureus	32.5
7	23.3 ± 7.2	23.3 ± 7.2	32.3 ± 8.7	–	1.4	*E. coli*	15.5
						P. aeruginosa	6.7
						B. contaminans	15.1
						S. aureus	41
8	6.6 ± 1.6	6.6 ± 1.6	8.5 ± 2.7	–	1.3	*E. coli*	125
						P. aeruginosa	86
						B. contaminans	125
						S. aureus	125
$AgNO_3$	26.4 ± 13	26.4	25.8 ± 5.0	–	1.0	*E. coli*	47
						P. aeruginos	39
						B. contaminans	74
							73
						S. aureus	

[a] IC_{50}, the concentration that causes the loss of 50 % cellular viability, upon 24 h exposure. [b] MIC, the lowest concentration (μg/mL) that inhibits bacterial growth. [c] Selectivity for cancer cells (SI = IC_{50} HDF/ IC_{50} A375). [d] Reported values for complexes: **1**,**5**,**6**,**7**, (Costa et al., 2021); **2**,**3**,**4**, $AgNO_3$ (Carvalho et al., 2019); **8** (Cardoso et al., 2017). [e] MBC values respectively: *E. coli* 62.5 μg/mL; *P. aeruginosa* 250 μg/mL; *B. Contaminans* 125 μg/mL; *S. aureus* 500 μg/mL.

Pseudomonas aeruginosa, *Staphylococcus aureus* and Burkholderia *contaminans*). Complexes **1** and **3,** with slightly higher IC_{50} values than **8,** display considerably higher antimicrobial activity. Among the complexes under study, complex **6** displays the lowest anticancer activity (31.4 ± 8.7 μM and 38.0 ± 7.3 μM for A375 and MeWo, respectively) but its antimicrobial activity against Gram negative strains is quite high. The cytotoxicity of the complexes for normal cells was ascertained using the mammalian fibroblasts HDF and V79, both widely used in toxicity testing. The results (Table 1) show that the IC_{50} values found for both HDF and V79 fibroblasts are in all cases higher than those for the A375 cells, a relevant aspect concerning the intended application. In addition, another interesting result was that, with few exceptions, the cell lines show different susceptibility to the cytotoxic effect of the complexes. The complexes are more cytotoxic toward the A375 cells.

From the complexes under study, complex **1** displays the best combined cytotoxic/antimicrobial properties and a reasonable selectivity (SI = 1.7). Thus, it was chosen to be incorporated in the HEMA-based hydrogel. Although, structure – activity relationships are out the scope of this work, the coordination polymer in addition to the hydrazone character of the camphorimine ligand in complex **1** (Costa et al., 2021) are structural aspects that conceivably play a role in its high anticancer/antibacterial activities. The cytotoxicity of a selection of silver camphorimine complexes analogous to complex **1**, was shown to rely on ROS (peroxides and superoxide) production in a dose-dependent manner with concomitant lipid peroxidation and cell membranes and other cellular components damaging.

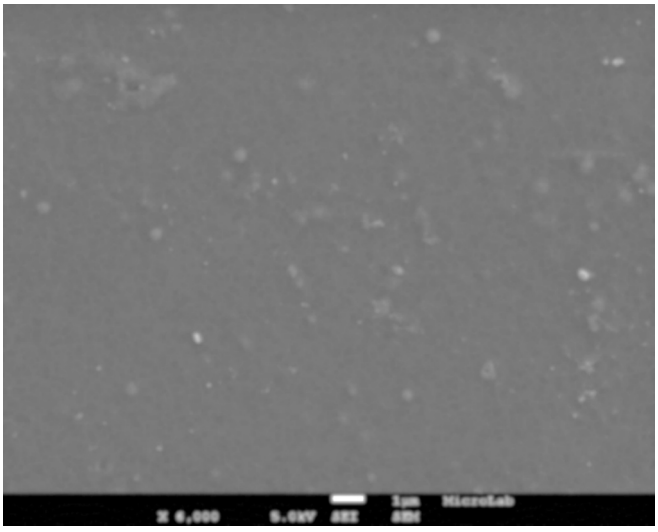

Fig. 2. SEM image of the HEMA-based hydrogels surface (×6000, scale bar 1 μm).

2.2. Characterization of the HEMA-based hydrogel

The HEMA-based hydrogel was characterized in terms of the most critical properties for wound dressing application.

Their surface morphology is depicted in the scanning electron microscopy (SEM) images (Fig. 2). A flat non-porous surface with small protuberances can be observed, in agreement with what was found in previous works for HEMA-based hydrogels. (Paradiso et al., 2015) Non-porous surfaces can minimize tissue adhesion, reducing trauma and pain during dressing changes. They also impair microbial infiltration while maintaining a moist environment favourable for healing.

The wettability and ability to absorb and retain water are essential properties to maintain the wound bed moisty and allow healing. (Maver et al., 2015) The values of the water contact angle with the HEMA-based hydrogel and its swelling ratio and water content and Young's modulus are depicted in Table 2. Data retrieved from mucoadhesion tests are also presented, namely, mucoadhesion force (F_{max}), displacement at the maximum force (S_{max}) and work of adhesion (W_{ad}). The errors are the ± standard deviations (in all cases n = 3, except for wettability n = 8 and Young modulus n = 5).

The produced HEMA-based hydrogels exhibit contact angles significantly lower than 90° reflecting the material' hydrophilic nature. The values of swelling ratio and water content, are within those found for other HEMA hydrogels (Teixeira et al., 2024) although lower than those reported for other wound dressing materials. (Minsart et al., 2022).

A moist environment was proven to facilitate the healing process of the wound by preventing dehydration and enhancing angiogenesis and collagen synthesis together with increased breakdown of dead tissue and fibrin. (Junker et al., 2013) However, excessive moisture may lead to tissue maceration, if the surrounding skin becomes overly moist and too soft, which can impair healing and increase the risk of infection. The proposed hydrogel presents a moderate water retention capacity (37.7 ± 0.13 %), sufficient to maintain a moist healing environment without promoting oversaturation or increasing the risk of wound maceration. In fact, commercial wound dressings with higher water contents (e.g., like Hydrosorb®, ~ 60 %), demonstrated to be suitable for treatment of light to moderate exuding wounds, supporting the tissue's granulation and epithelialization and promoting the debridement of necrotic parts. (Minsart et al., 2022) The water content of conventional hydrogels, as the HEMA-based studied in this work, also determines their oxygen permeability, as oxygen diffuses through the aqueous phase of the polymer matrix. (Teixeira et al., 2024) Oxygen plays a critical role in chronic wound healing, since it enhances collagen synthesis, angiogenesis, immune function, and cell proliferation, essential for tissue repair and infection control. (Schreml et al., 2010) Therefore, by maintaining hydration, the hydrogel will present some gas exchange capacity, even in the absence of surface porosity. Although this figure is not as high as desired, the use of occlusive dressings (e.g. hydrocolloids) in the management of chronic wounds is not uncommon (Nguyen et al., 2025) due to their ability to maintain a moist wound environment, absorb exudate and reduce pain during dressing changes. However, their use requires careful consideration of the specific characteristics of the wound and the needs of the patient. In any case, a close follow up of the state of the wound is mandatory, with regular monitoring and dressing changes, to ensure the best progression.

Table 2
Physical characteristics of the HEMA-based hydrogels.

Water contact angle (∘)	48.9 ± 0.2
Swelling ratio (%)	60.6 ± 0.4
Water content (%)	37.7 ± 0.13
Young modulus (kPa)	568.4 ± 89.9
F_{max} (mN)	121.7 ± 15.3
S_{max} (mm)	0.65 ± 0.02
W_{ad} (mJ)	0.32 ± 0.03

In what concerns the mechanical properties, tensile tests were conducted to evaluate the materials' stiffness. The value obtained for the Young' modulus (568.4 ± 89.9 kPa, Table 2) falls within the range reported for commercial wound dressings (240–950 kPa) allowing the handling of the material during application without any issues. (Minsart et al., 2022).

The results of the frequency sweep analysis conducted to a fixed shear strain of 0.1 % for the HEMA-based samples as displayed in Fig. 3. As expected, the storage modulus (G') consistently exceeds the loss modulus (G''), indicating predominantly elastic behavior. This solid-like structure is ideal for handling during application without tearing. The observed values are consistent with those reported for similar HEMA-based hydrogels (Meakin et al., 2003) and other hydrogels developed for similar applications. (Rahmani et al., 2020; Rainho et al., 2025).

Ensuring a low adhesion of the dressings to the wound tissues is crucial to minimize pain and tissue damage during dressing changes. In fact, dressing adhesion can disrupt newly formed tissue and delay wound healing, increasing the risk of infection and complications. Thus, the strategy commonly adopted is the application of the therapeutic dressings followed by a second dressing fixed to the healthy skin that surrounds the wound. This secures the primary dressing in place, helps to maintain a controlled healing environment on the wound preventing contamination, and protects it from external mechanical stress. A mucoadhesion assay was conducted to test the hydrogel detachment from pig small intestine inner membrane, which is often used to mimic the mucous-like texture of the wound. (Singh et al., 2013) The values of the mucoadhesion force (F_{max}) as well as of the displacement at the maximum force (S_{max}) and work of adhesion (W_{ad}) are displayed in Table 2. Such values reflect the samples' ability to softly adhere to the wound and are of the same order of magnitude of those found for low adhesive commercial dressings like polyurethane Hydrosorb Comfort gel pad and Urgocell Silver AG Plata. (Klode et al., 2011).

2.3. In vitro release tests

The hydrogels were loaded by soaking in a solution of complex **1**. Then, before performing the *in vitro* release tests, a sterilization method was selected to ensure that the wound dressings not only will be safe from the biological point of view when placed in the wound but also will be able to release the bioactive agent in a sustained way, during a suitable time (at least 24 h) and in adequate amounts. Moreover, the sterilizing process should not impair the therapeutic activity of the complex. Sterilization methods, such as gamma irradiation or steam sterilization, are widely used in the sterilization of wound dressings, however, when the dressings contain sensitive compounds (as complex **1**), alternative methods must be employed to preclude their degradation by ionizing radiation or high temperature. The use of high hydrostatic pressure (HHP) combined with moderate temperatures to sterilize drug-loaded hydrogels was successfully explored in previous works (Topete et al., 2020) and effectively employed to sterilize biological tissues during the decellularization process, representing a promising approach for the production of tissue-derived healthcare products. (Pires et al., 2022; Otaka et al., 2024) HHP is widely used in food industry as a nonthermal pasteurization method, (Buzrul, 2015; Dong et al., 2021) but it is still scarcely used in the sterilization of medical devices. HHP uses relatively moderate/high temperatures (typically 70 °C or above) and extremely high pressures (commercially up to 600 MPa) to kill/inactivate the microorganisms without affecting the drugs' integrity and only causing slight changes in the hydrogel's properties.

In the present study, the influence of HHP on the pattern of release of complex **1** from the HEMA-based hydrogel, was evaluated through *in vitro* release experiments carried out in static sink conditions, before and after HHP sterilization. The cumulative release profiles are shown in Fig. 4.

The analysis of the results shows that in both cases the complex was released (≈ 90 %) in the first 8 h and was practically not affected by the

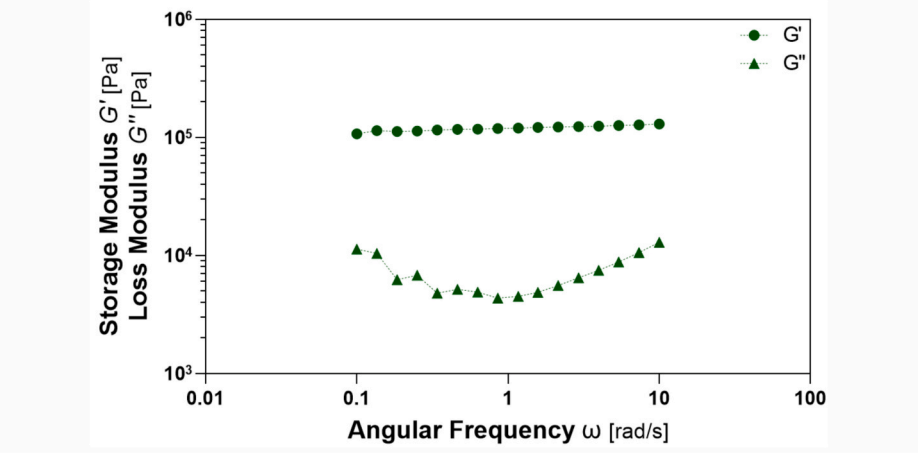

Fig. 3. Frequency sweep (0.1–100 rad/s) analysis of the storage (G') and loss (G'') moduli for the HEMA based-hydrogels, at a fixed strain rate $\gamma = 0.1$ %. The error bars show the standard deviation (n=±3).

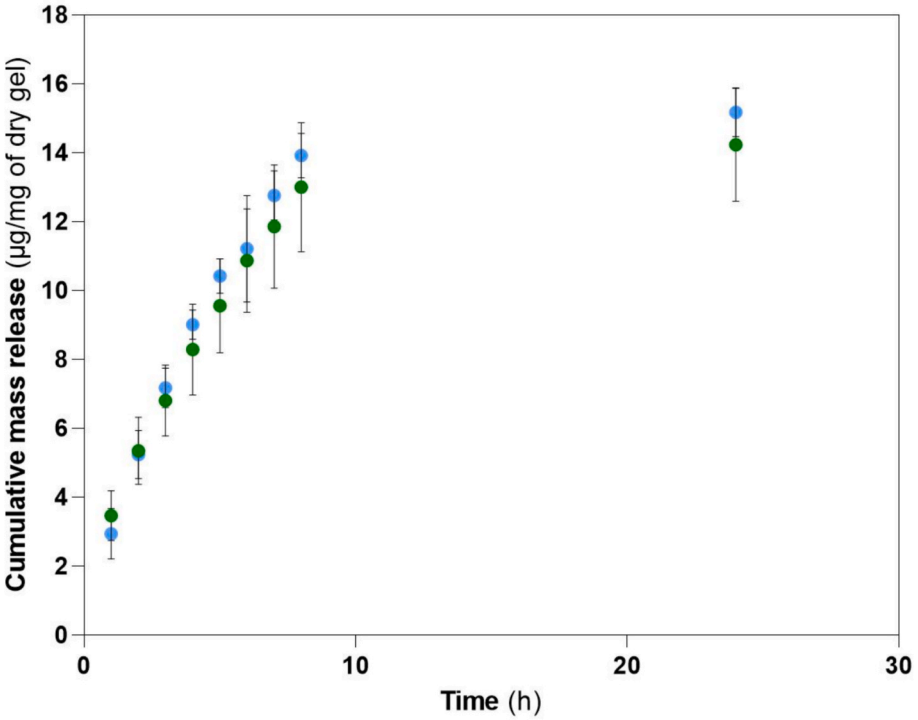

Fig. 4. Cumulative mass release of complex **1** from non-sterilized (green symbols) and HHP sterilized (blue symbols) HEMA-based hydrogels. Error represents the ± standard deviations (n = 4). (For interpretation of the references to colour in this figure legend, the reader is referred to the web version of this article.)

sterilization procedure, since the release profiles are quite similar with a slightly higher total amount of compound being released (15.18 ± 0.69 µg/mg dry gel) after 24 h HHP sterilization *versus* to the non-sterilized samples (14.23 ± 1.52 µg/mg dry gel). Such pattern suggests that HHP does not significantly affect the structure of the hydrogel, and therefore its properties. It shall be stressed that although static conditions may lead to a relatively rapid drug diffusion, the physiological conditions of the wound (where the exudate is gradually produced and reabsorbed by the tissues or by the dressing) are expected to support a prolonged and controlled release, aligning with the therapeutic goals of chronic wound management. The design of an experimental setup to simulate this behavior *in vitro* is difficult, since the wound hydrodynamic conditions can vary significantly.

To get insight into the complex release mechanism from the sterilized material, the cumulative release profile (up to 60 % of the total release) was fitted to the Korsmeyer-Peppas equation: (Ritger and Peppas, 1987)

$$\frac{M_t}{M_\infty} = kt^n \quad (1)$$

where M_t and M_∞ are respectively, the mass released at time t and as time tends to infinity, k is a *pseudo*-kinetic constant and n is the diffusional exponent. The fitting (done with Table Curve 2D v5.0 software) led to $k = 0.1886$ and $n = 0.9273$, with a correlation coefficient $R^2 = 0.9999$, which demonstrates that the model is particularly suitable to describe the drug release behavior. The fact that n assumes a value higher than 0.5 shows the occurrence of non-Fickian diffusion.

Considering that the average weight of the dry hydrogel samples is 32 mg, and that their diameter is 10 mm, it can be concluded that the

total amount of complex released from the sterilized samples is 618.5 μg/cm^2 (24 h). The efficacy of the dressing in terms of antibacterial and anticancer activities shall depend on several factors, like the type of bacteria that may colonize the wound, the kind of cancerous cells, and the exudate composition and volume. The exudate characteristics depend on the wound type, existence and extension of the infection, biofilm formation, inflammatory response and tissue oxygenation. The patient's systemic conditions (e.g., diabetes or poor circulation), age, nutritional status, and medication also may affect the exudate production. Highly exuding wounds can be expected to lead to lower concentrations of the bioactive agents when these are released from the dressings into the wound bed, which could compromise the efficacy of the treatment. Dealey *et al.* (Dealey et al., 2013) used two distinct methods to quantify the production of exudate by chronic wounds. The evaluation of several types of wounds (e.g. diabetic foot ulcers, leg ulcers, wounds with drained abscesses and necrotic lacerations), non-infected and infected with different microorganisms, showed that the exudate production determined by dressing weighing before and after contact with wound did not exceed 0.21 g/cm^2 in 24 h, while the exudate collected in topical negative pressure therapy was in average 1.3 g/cm^2 in the same period. They compared these values with the ones obtained by other authors for the exudate production rate, finding a good agreement (0.42–0.86 g/cm^2 in 24 h. (Ferguson et al., 1991; Thomas et al., 1996) The Consensus Document of the World Union of Wound Healing Societies "Wound Exudate, effective assessment and management, (Harding, 2019) gathers values obtained in other studies, but all of them are of the same order of magnitude. A wound that produces 1 g/cm^2 of exudate *per* day (or 1 mL/cm^2 *per* day, since exudate density is close to 1 g/mL (Slack, 2020) shall origin drug concentrations 11–28 times superior to the MICs of the different bacteria referred in Table 1 (being the lowest value for *S. aureus* and the highest for *E.coli*), which revealed to be more resistant to complex **1**). If instead of MIC we consider the MBC values *(E. coli* 62.5 μg/mL; *P. aeruginosa* 250 μg/mL; *B. Contaminans* 125 μg/mL; *S. aureus* 500 μg/mL*),* the concentration will be 1 to 10 times higher. This means that the produced wound dressings besides inhibiting the microbial growth, shall also have capacity to kill the microorganisms. Regarding the A375 cells, the obtained concentration for the considered volume of exudate can reach a value 160 times higher than the correspondent IC_{50} (the molecular weight of complex **1** is 350 g/mol), also confirming the efficacy of the dressings in terms of anticancer activity. Due to the complexity of the factors involved, only *in vivo* tests would allow to confirm the real therapeutic potential of the dressings.

2.4. Compound 1 integrity confirmation

To ascertain on the integrity of the complex released from the hydrogel matrix after sterilization, a sample was collected (8 h) and purified by HPLC, to separate NaCl from the complex. Thereafter, the purified solution was evaporated to obtain a powder, which was analyzed by cyclic voltammetry. The cyclic voltammogram of the sample obtained from the HEMA hydrogel-complex-**1** system (Fig. 5, red), fully agrees with that of the original complex **1** (Fig. 4, black) showing the Ag(I)→Ag(0) reduction (wave I) at the expected values of potential and a similar electrochemical behavior in what concerns adsorption at the Pt electrode (wave A). Such pattern corroborates the integrity of the complex upon HHP sterilization and release. The relative intensities of the waves reflect the concentration of the samples.

2.5. Antibacterial activity of hydrogels

The antibacterial activity of hydrogels empty or loaded with complex **1** was determined by enumerating the colony forming units of *E. coli*, *P. aeruginosa*, *B. contaminans*, and *S. aureus* after incubation of hydrogel disks for 24 and 48 h, in 1 mL MH inoculated with 5 × 10^5 CFU/mL of each strain, and contained in the wells of 24-well plates at 37 °C (see experimental). The results obtained are summarized in Table 3.

As shown in Table 3, the hydrogel disks did not present any antibacterial activity, as values of CFUs after incubation for 24 h were about 3–4 logs higher than the initial CFUs (5 × 10^5). However, the presence of hydrogel disks loaded with complex **1** led to the complete reduction of the initial CFUs from 5 × 10^5/mL to 0 in the case of tested Gram-

Table 3
Antibacterial activity of hydrogel disks loaded with complex **1**.

	Hydrogel Disk	Hydrogel Disk loaded with Complex **1**	
	24 h	24 h	48 h
E. coli ATCC25922	5.4 ± 2.6 × 10^8	0	0
P. aeruginosa 477	2.3 ± 1.3 × 10^9	0	0
B.contaminans IST408	5.1 ± 2.8 × 10^8	0	0
S. aureus Newman	9.0 ± 1.0 × 10^8	2.0 ± 1.0 × 10^3	> 10^7

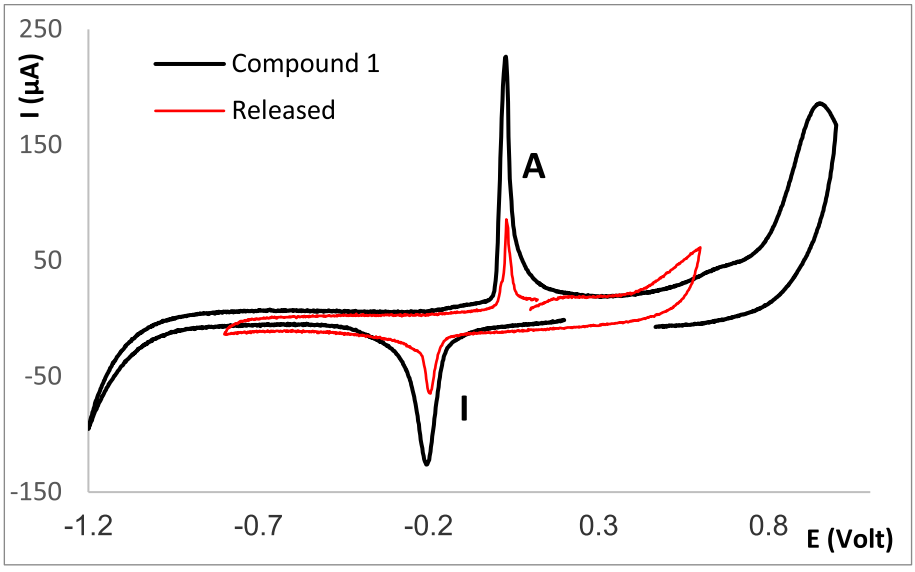

Fig. 5. Cyclic voltammograms of the complex **1** (original, black) upon release from the HEMA hydrogel (red). (For interpretation of the references to colour in this figure legend, the reader is referred to the web version of this article.)

negative bacteria *E. coli*, *P. aeruginosa* and *B. contaminans*. In the case of *S. aureus*, a reduction of the initial CFUs from 5×10^5/mL to 2×10^3/mL (more than 99 %) was registered after 24 h. After 48 h, no inhibitory effect of complex **1** towards S. aureus was observed. This might be attributed to the loss of activity of complex **1** that display MIC values towards *S. aureus* much higher than for *E. coli*, *P. aeruginosa* and *B. contaminans* (Table 1).

2.6. Biocompatibility tests

The irritation potential and hemocompatibility of the hydrogels are characteristics that must be evaluated when developing new wound dressings.

To infer about the irritation potential of the complex loaded HEMA-hydrogel samples, the Hen's Egg test on the chorioallantoic membrane (HET-CAM) was performed. This test is widely employed in the development of materials intended for skin and mucosal applications, including wound dressings, being an alternative to traditional animal testing. It consists in the evaluation of vascular reactions (such as hemorrhage, lysis, and coagulation), induced by the samples on the chorioallantoic membrane of fertilized eggs. Fig. 6a, shows that the sample loaded with the complex did not lead to any irritability sign on the CAM after 5 min of exposure (IS = 0.0 ± 0.0). The results were similar to that of the negative control (Fig. 6b), thus the samples can be classified as non-irritant. As expected, the positive control led to severe irritability, demonstrating all signs of irritancy (Fig. 6c), with an IS = 20.5 ± 0.7.

Regarding hemocompatibility, tests were conducted to determine the hemolysis ratio when the complex loaded samples were put in contact with suspensions of blood cells. The obtained value (0.100 ± 0.04 %) is much lower than the maximum value (5 %) defined by the standard (ISO 10993–4) to ensure hemocompatibility (5 %), (Iso, 2017) so the loaded samples are safe to be used in contact with blood.

3. Conclusions

Eight silver camphorimine complexes of five distinct families ([Ag$(NO_3)(^AL)_n$] (n = 1,2); [Ag$(NO_3)(^BL)_2$]; [Ag$(NO_3)(^CL)$]; [Ag$(OH)(^BL)$]) were assessed for their cytotoxic activity against melanoma cells A375 and MeWo and toxicity against normal fibroblasts HDF and V79. The IC_{50} values show that all the complexes display good anticancer activity at short incubation time (24 h) with acceptable toxicity in the normal fibroblasts. Combining these data with the former published results on the antibacterial properties of the complexes, complex **1** was selected as having the best combined anticancer/antibacterial activities and selectivity for incorporation in a HEMA-based hydrogel.

The hydrogel was characterized in view of the most relevant properties regarding the use as wound dressing. The results showed that the properties fulfil the use foreseen since it is hydrophilic and, despite the non-porous morphology, it can retain a significant amount of water which is a critical characteristic to ensure a moist wound. The stiffness of the material was similar to that of the commercial dressings, ensuring safe handling (without tearing) and good conformability with the wound. The results from the mucoadhesion tests show that the dressings are not expected to cause mechanical damage to the wound in the changing procedure.

The sterilization process by HHP did not induce meaningful differences in the drug release profiles, which suggests that the structure and properties of the hydrogel were not affected by the sterilization procedure. The integrity of the complex upon loading in the hydrogel and sterilization through HHP was corroborated by cyclic voltammetry.

Drug release studies revealed that the complex followed a non-Fickian diffusion release mechanism. The amount released and release-kinetics shall ensure an effective antibacterial activity, during at least 24 h, against Gram-negative *E. coli*, *P. aeruginosa* and *B. contaminans* as well as Gram-positive *S. aureus*.

Moreover, the achieved complex concentrations are also enough to guarantee an anticancer effect against A375 cells. Biocompatibility tests indicated that the drug loaded material is non-irritant and hemocompatible.

The overall results of this study show that the HEMA-based hydrogel loaded with complex **1** is a promising candidate for wound dressing applications, particularly for chronic wounds with risk of bacterial infection and malignant transformation. However, further studies are needed, in particular *in vivo* studies, to assess its long-term efficacy and validate its clinical potential to prevent infections and assure an anticancer effect.

4. Experimental

4.1. Materials

2-hydroxyethyl methacrylate (purity ≥ 99 %, HEMA), ethylene glycol dimethacrylate (purity ≥ 98 %, EGDMA), 2,2′-azobis(2-methylpropionitrile) (purity ≥ 98 %, AIBN), phosphate buffered saline (PBS) tablets, dimethyl sulfoxide (DMSO, purity ≥ 99.9 %), ethanol (,96 %) and sodium chloride (NaCl), were provided by Sigma-Aldrich (Germany). Poly vinylpyrrolidone (PVP) Kollidon (Cardoso et al., 2017) was provided by BASF (USA). Sodium hydroxide (NaOH, purity ≥ 99 %) was obtained from Merck (USA). Toluene (Reag. Ph. Eur., purity ≥ 99.5 %) was obtained from Panreac (Spain). Ultrapure water (resistivity > 18 MΩcm) was obtained from a Millipore system and used to prepare all solutions.

4.2. Complex synthesis

All the complexes were synthesized under nitrogen using Schlenk and vacuum techniques. Complexes **1**–**8** (see Table 1) were prepared according to reported procedures. (Costa et al., 2021; Carvalho et al., 2019; Cardoso et al., 2016) The purity of all complexes was confirmed by elemental analysis obtained at the accredited IST-Analysis Laboratory (LAIST)) and ^1H and ^{13}C NMR obtained from CD_3CN or DMSO solutions using Bruker Avance II+ (300 or 400 MHz) spectrometers (Bruker BioSpin AG, Industriestrasse (Tang et al., 2010); Fällanden, Switzerland. The NMR chemical shifts are referred in TMS ($\delta = 0$ ppm).

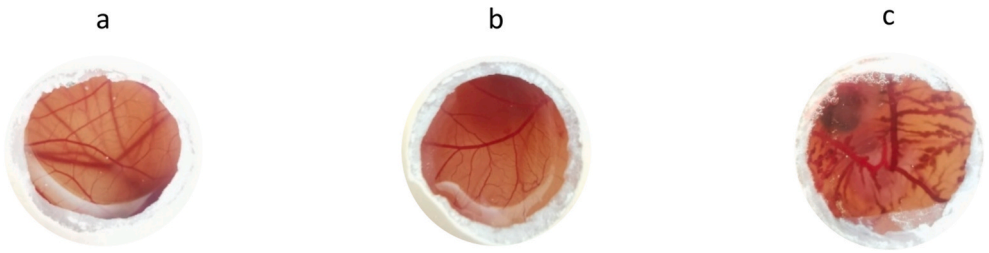

Fig. 6. CAM photographs after 5 min exposure to the complex loaded HEMA-based hydrogels (a), negative control (NaCl 0.9 %) (b) and positive control (NaOH 0.1 M) (c).

4.3. Cyclic voltammetry

A three-compartment cell equipped with Pt wire working and secondary electrodes interfaced with a VoltaLab PST050 equipment was used. The cyclic voltammograms were obtained under dinitrogen, at 200 mV/s, from water (Millipore) / NH_4BF_4 solutions (0.10 M) used as electrolyte. Prior to addition to the electrolyte solution (2.5 mL), complex **1** was dissolved in DMSO (3.0 mg/50 μL) and the solution added to 500 μL de DMEM. The window of potential was established using a solution of the freshly prepared electrolyte. The cyclic voltammogram of the "released" was obtained from the hydrogel released solutions (8 h) under the same experimental conditions used for the pure complex.

4.4. Hydrogel production

The HEMA-based hydrogel was prepared by dissolving EGDMA (81 mM), PVP (1.3 mM), and AIBN (12 mM) in a 1:1 vol ratio solution of HEMA and distilled and deionized (DD) water. The components were dissolved in the aqueous solution under continuous magnetic stirring. To avoid the formation of bubbles during polymerization, the solution was degassed by bubbling a gentle stream of nitrogen for 2 min, followed by a 5 min ultrasonic bath. The polymerization was achieved by placing the solution in a mold (composed by two silanized glasses, separated by a polyurethane frame) in front of a UV-lamp (UV – Exposure box 2, 350 nm, 230 W/4 × 15 W, Gie-Tec GmbH, Eiterfeld, Germany) for 100 min, at a distance of 15 cm. The hydrophobization of the glass molds was previously carried out by brushing a tin film of toluene and letting it evaporate for 2 h in a flow chamber, followed by a rinse with ethanol. After polymerization, to remove undesirable and toxic unreacted monomers and impurities, the samples were exposed to an extensive washing protocol (DD water for 5 days, changed 3 times a day). The samples were cut in the hydrated state with different dimensions, depending on the requirements for each analysis/characterization method. The cut samples were dried in an oven for 24 h at 36 °C and afterwards stored.

4.5. Hydrogel characterization

4.5.1. Morphology analysis

Hydrated samples (8 mm diameter) were first frozen by immersion for 5 s in liquid nitrogen (≈-196) and immediately placed in a lyophilizer (Freeze-dryer Alpha 1–2 LDPlus, Gefriertrocknungsanlagen GmbH, Germany) at approximately −60 °C and 0.008 Pa for 24 h. This process was carried out to conserve morphology of the hydrated samples. The surface morphology of the lyophilized hydrogel was analyzed by SEM (Hitachi S2400, Chiyoda, Tokyo, Japan) at 3000 × and 6000 × magnifications. To overcome the non-conductive nature of the polymeric material, before the analysis it was coated with a gold/palladium (Au/Pd, 20:80) film in a sputter coater (Q150T ES, Polaron, Quorum Technologies, UK).

4.5.2. Rheological properties

Rheological tests were performed using a Modular Compact Rheometer (MCR92, Anton Paar, Austria) at 34 °C, employing a 25 mm diameter parallel plate (PP25) rotational geometry. The thickness of each hydrogel disk was measured prior to placement on the preheated stationary lower plate. To prevent dehydration, a few drops of deionized and distilled (DD) water were added around the sample. The upper plate was lowered to approximately 98 % the hydrogel's thickness, slightly compressing the sample. An amplitude sweep test was first conducted at a constant frequency of 1 Hz to identify the linear viscoelastic regime (LVER), defined as the strain range where the hydrogel maintains its elastic behavior. Subsequently, a frequency sweep test was carried out using a constant strain within the LVER and an angular frequency range of 0.1–100 rad/s. All frequency sweep tests were performed in triplicate.

4.5.3. Wettability

The wettability of the hydrated hydrogel was studied using the captive bubble method. The samples were placed upside-down and completely immersed in DD water, in a liquid cell. Air bubbles were carefully produced over the sample surface with a syringe with an inverted cane-shaped needle. At pre-defined times, pictures of the bubbles were taken by a video camera (jAi CV-A50, Spain) attached to a microscope (Wild M3Z Leica Microsystems, Germany). The obtained images were analyzed with the ADSA-P software (Applied Surface Thermodynamics Research Associates, Toronto, Canada). Eight measurements were done with independent bubbles.

4.5.4. Water content and swelling ratio

To evaluate both the water content and water swelling ratio of the HEMA-based hydrogels, samples were weighed in their dry state (W_d) and placed in Falcon® tubes with 3 mL of DD water. At pre-established times they were carefully removed from the tubes, blotted with lab paper and weighted (W_h). The assays were performed in triplicate. The following equations were used to determine the water content and swelling ratio, respectively. (Li et al., 2009)

$$watercontent\,(\%) = \frac{W_h - W_d}{W_h} \times 100 \quad (2)$$

$$swellingratio(\%) = \frac{W_h - W_d}{W_d} \times 100 \quad (3)$$

4.5.5. Mechanical assays

The samples were cut with dumbbell-shape (2.5 mm maximum width and 6 mm gauge length), and their thickness was measured with a caliper prior to tensile test. This test was done in a Texture analyzer (TA. XT Express Texture Analyser, Stable Micro Systems, Surrey, UK), with a speed of 0.3 mm/s until rupture. Stress/strain curves were obtained using the software TE32LiteExpress and the Young' modulus was calculated over a strain range between 1 and 10 %. The analysis was done in sextuplicate.

4.5.6. Mucoadhesion

To evaluate the samples mucoadhesion properties, the samples were put in contact with pig small intestine (purchased to Talho "Luso Francês", Lisboa, Portugal). First the intestine was carefully washed with DD water and cut with a scalpel to expose the mucosa membrane. This was placed on a platen connected to the Texture Analyzer and a small amount of DD water was dropped on the top of the membrane to avoid its dehydration. Hydrated samples (10 mm of diameter) were glued to the top platen of the equipment. The test was started by promoting direct contact between the mucosa and the hydrogel, with an applied force of 0.05 N for 10 sec. Detachment was promoted by moving up the hydrogel at a speed of 0.5 mm/sec. From the plotted curve (force *versus* distance) the maximum mucoadhesion force (F_{max}), displacement at maximum force (S_{max}) and work of adhesion (W_{ad}, area under the curve) were determined using the software TE32LiteExpress. The experiments were done in triplicate.

4.6. Complex loading and release from the produced hydrogels

The hydrogel samples (10 mm of diameter, n = 4) were placed individually in Falcon® tubes with 3 mL of complex **1** solution (1.5 mg/mL in NaCl 0.9 %, 1 %v/v DMSO), and left at room temperature for 72 h, protected from light. After loading, the samples were carefully removed from the tubes, blotted with lab paper and placed in vials containing 3 mL of NaCl (0.9 %). The closed tubes were placed in an incubating orbital mini shaker (VWR® Incubating Mini Shaker, Avantor, USA) at 36 °C for 48 h, at 180 rpm. At selected times, aliquots (200 μL) were taken from each tube and replaced by fresh NaCl solution. Complex concentration quantification was carried out by HPLC, measuring the

area of the peak correspondent to the complex. The analysis was performed on a Varian ProStar equipment, containing a UV detector set at 254 nm and a C18 column (Varian Microsorb-MV, 250 mm × 4.6 mm, 5 μm). The mobile phase (acetonitrile/water acidified with formic acid 0.1 %) was fed at a flow rate of 1 mL/min. The injection volume was 20 μL for the calibration and release curves, and 100 μL for collecting the fractions of the purified complex (retention time of 11.5 min) used for cyclic voltammetry. The standards for calibration were prepared at concentrations of 0.5, 0.25, 0.125, 0.0625, 0.0313 and 0.0156 mg/mL. The calibration curve was adjusted to Area = 10835xConcentration with an excellent linearity ($R^2 = 0.999$).

4.7. High hydrostatic pressure sterilization

To ensure biological safety the samples were subjected to a sterilization process by high hydrostatic pressure (HHP). The dry samples were first packed in polyamide + polyethylene bags with 3 mL of complex solution (1.5 mg/mL in NaCl 0.9 %, 1 %v/v DMSO). The packed samples were pre-heated in a water bath at 70 °C for 5 min and then placed on a pre-heated (70 °C) polypropylene basket for thermal insulating purposes and sterilized using a pilot-scale high-pressure equipment (Hiperbaric (Harding, 2019); Hiperbaric S.A., Burgos, Spain) at 600 MPa for 10 min at 70 °C. After processing, the bags with the samples were immediately removed from the basket and cooled down with room-temperature water. The sterilization procedure took place on the same day of loading.

4.8. Biological tests

4.8.1. Irritability

The Hen's egg test – chorioallantoic membrane (HET-CAM) was used to evaluate possible irritation induced by the loaded samples. Chicken eggs were purchased from Sociedade Agrícola da Quinta da Freiria, SA (Portugal) and incubated for 8 days in an egg incubator (HHD incubator model YZ-56S, China) at 36.7 ± 0.4 °C with 60 ± 3 % relative humidity. After incubation, the eggs were individually removed from the incubator and their eggshell was removed using a rotary saw (Dremel 3000, Breda, Netherlands) to expose the inner membrane. This was hydrated with a few drops of NaCl 0.9 %, and the eggs were left in the incubator for an additional half an hour. The hydrated inner membrane was carefully removed from the top of the CAM with a tweezer. Complex **1** loaded samples (n = 3) were directly placed on the CAM, and monitored for any possible signs of irritability (i.e., lysis, haemorrhage and coagulation) for 5 min. The time of appearance of any of the above-mentioned signs was registered to classify the systems according to the irritation score (IS) classification:

$$Irritationscore(IS) = \left[5 \times \left(\frac{301 - T_1}{300}\right) + 7 \times \left(\frac{301 - T_2}{300}\right) + 9 \times \left(\frac{301 - T_3}{300}\right)\right] \quad (4)$$

where T_1, T_2, T_3 represent the time (in sec) necessary to appear haemorrhage, vascular lysis and coagulation, respectively. Experiments were carried in triplicate.

A negative and a positive control were obtained by adding to the CAM 300 μL of NaCl 0.9 % and NaOH (0.1 M), respectively. Experiments were carried in triplicate.

4.9. Hemocompatibility

Blood samples were collected from healthy volunteers via venepuncture in sodium citrate anti-coagulant vacutainer tubes (BD Vacutainer®, Plymouth, UK) under aseptic conditions in Serviços de Saúde of Instituto Superior Técnico, Lisbon, after obtaining informed consent (Approved by the Ethical Committee of Egas Moniz – Ref. n◦1047/2022).

HEMA-based hydrogel samples (10 mm diameter, n = 4) loaded with complex **1** were placed into sterile Falcons® tubes with 200 μL of blood and 2 mL of PBS. Two controls were also made by adding the same volume of blood to 2 mL of PBS (negative control, C-) and to 2 mL of DD water (positive control, C +). PBS and DD water used during this assay were sterilized through steam heat in an autoclave for 20 min at 121 °C.

The tubes were closed and incubated for 1 h at 37 °C, protected from light. After incubation, the hydrogels were carefully removed from the tubes, and these were centrifuged at 3000 rpm for 10 min. Aliquots (200 μL) of the supernatant were collected, and the respective absorbance was measured at 540 nm, using a UV/Vis spectrophotometer (ThermoFisher Multiskan Go, Thermo Fisher Scientific, USA). Eq. (5) was used to determine the hemolysis ratio. (Garcia et al., 2023)

$$Hemolysis(\%) = \frac{abs_s - abs_{C-}}{abs_{C+} - abs_{C-}} \quad (5)$$

where abs_s is the sample' absorbance measured, and abs_{C-} and abs_{C+} are the absorbance measured for the negative and positive controls, respectively. Experiments were done in triplicate.

4.9.1. Cytotoxicity assays

The human melanoma A375 and MeWo cells were obtained from ATCC (CRL-1619) and ATCC (HTB-65), respectively. The human dermal fibroblasts HDF and the hamster lung fibroblasts V79 were obtained from Sigma-Aldrich and ATCC (CCL-93), respectively. For the cytotoxicity assays, the melanoma and V79 cells were cultured in DMEM + GlutaMAX™ (Thermo Fisher Scientific, Inc., USA) supplemented with 10 % fetal bovine serum (FBS) (Thermo Fisher Scientific, Inc., USA) and maintained at 37 °C in a 5 % CO_2 humidified atmosphere. The human fibroblasts were grown in Fibroblast Growth Medium (Sigma-Aldrich). Fresh stock solutions (10 mM) of the compounds were prepared in DMSO, except for the silver salt $AgNO_3$ that were prepared in distilled water. Serial dilutions from the stock solutions were done in each cell medium. The cellular viability was measured by the colorimetric MTT assay as described. (Costa et al., 2022) In a typical assay, cells were seeded in 96-well plates at a density of approx. 10^4 cells/200 μl in each appropriate medium and left to incubate for 24 h for optimal adherence. Then, the medium was discarded and 200 μl of each serial dilution of compounds in fresh medium were added to the cells. The incubation was carried out at 37 °C for 24 h. At the end of treatment, the compounds solutions were discarded, and the cells were incubated with 200 μl of MTT solution in PBS (1.2 mM). After 3 h at 37 °C, the medium was removed and replaced by 200 μl of DMSO to solubilize the formazan crystals formed. The percentage of cellular viability was evaluated measuring the absorbance at 570 nm using a Varioskan LUX scanning multimode reader (Thermo Fisher Scientific, Waltham, MA, USA). The IC_{50} values were calculated from dose-response curves using the GraphPad Prism software (version 6.0). Results are mean ± SD of at least two independent experiments done with six replicates.

4.9.2. Hydrogel antibacterial activity

The antibacterial activity of hydrogels loaded with complex **1** was tested against the bacterial strains *Escherichia coli* ATCC25922, *Pseudomonas aeruginosa* 477, *Burkholderia contaminans* IST408, and *Staphylococcus aureus* Newman. For this purpose, bacterial cultures were grown overnight at 37 °C in Lennox Broth liquid medium (Sigma-Aldrich, St. Louis, USA) with orbital agitation. Adequate volumes of cultures were then added to 1 mL of Mueller-Hinton broth contained in 24-wells plate to obtain 5 × 10^5 colony forming units *per* mL. One hydrogel disk containing complex **1** was then poured in each well. An aliquot of 100 μL was taken from each well, after 24 and 48 h of incubation, adequately serially diluted 1:10, and 100 μL. The adequate dilutions were spread onto the surface of solid LB medium. The inoculated plates were incubated for 24 h at 37 °C, time after which the CFUs formed onto the plates

surface were enumerated. At least 4 hydrogel disks were used for each bacterial strain. Control experiments with hydrogel disks without complex 1 were also performed as described above.

4.10. Minimal Bactericidal Concentration (MBC)

The MBC of complex **1** towards the bacterial strains under study (*E. coli*, *P. aeruginosa*, *B. contaminans*, and *S. aureus*) was performed based on microdilution method as described before. (Costa et al., 2021; Carvalho et al., 2019) For this purpose, a 10 mg/mL stock solution of complex **1** in DMSO was prepared. Aliquots of 20 μL of the stock solution were added to 180 μL of Mueller-Hinton (MH) liquid medium contained in the wells of a microtiter plate. From this initial concentration (1000 μg/mL), serial 1:2 dilutions were carried out in MH liquid medium. To the 100 μL of serially diluted complex **1** solutions in MH contained in the wells, 100 μL of bacterial cultures containing 10^6 colony forming units were added. After 24 h of incubation at 37 °C, aliquots of 100 μL from wells exhibiting no bacterial growth were spread onto the surface of LB solid medium. MBC was considered as the minimal concentration of complex **1** for which no bacterial colonies were detected after 24 h of incubation at 37 °C. The maximal concentration of DMSO was 5 % (V/V), compatible with bacterial growth Fontinha et al. (2020). Experiments were carried out in quadruplicate for each bacterial strain.

CRediT authorship contribution statement

Joana P. Costa: Validation. **Diana C. Silva:** Validation. **Fernanda Marques:** Validation, Investigation. **Jeremias Muazeia:** Investigation. **Jorge H. Leitão:** Investigation. **Carlos A. Pinto:** Formal analysis. **Jorge A. Saraiva:** Formal analysis. **Ana P. Serro:** Writing – review & editing, Validation, Methodology, Conceptualization. **M.Fernanda N.N. Carvalho:** Writing – review & editing, Validation, Conceptualization.

Funding

Funding through projects of CQE – Centro de Química Estrutural https://doi.org/10.54499/UIDB/00100/2020 and https://doi.org/10.54499/UIDP/00100/2020); Associate Laboratory IMS – Institute of Molecular Sciences (https://doi.org/10.54499/LA/P/0056/2020);

CiiEM – Centro de Investigação Interdisciplinar Egas Moniz (https://doi.org/10.54499/UID/BIM/04585/2020);

Associated Laboratory LAQV-REQUIMTE (UID/50006 – Laboratório Associado para a Química Verde – Tecnologias e Processos Limpos); Research project Milk4WoundCare (https://doi.org/10.54499/2022.03408.PTDC);

Diana C. Silva for Junior Research contract FCT (https://doi.org/10.54499/2022.08560.CEECIND/CP1713/CT0016) and a PhD grant to Joana P. Costa (https://doi.org/10.54499/UI/BD/152244/2021).

Fundação para a Ciência e Tecnologia, through the project UID/Multi/04349/2020 (C^2TN).

Project 2023.13256.PEX, IBB—Institute for Bioengineering and Biosciences for projects UIDB/04565/2020 and UIDP/04565/2020, and i4HB (project LA/P/0140/2020).

Declaration of competing interest

The authors declare that they have no known competing financial interests or personal relationships that could have appeared to influence the work reported in this paper.

Acknowledgment

The Portuguese NMR IST–UL Centers and ChemBioLab for facilities.

Data availability

Data will be made available on request.

References

Bayramoğlu, G., Batislam, E., Arica, M.Y., 2009. Preparation and drug-release behavior of minocycline-loaded poly[hydroxyethyl methacrylate-*co*-poly(ethylene glycol)–methacrylate] films. Appl. Chem. 112, 1012–1020. https://doi.org/10.1002/app.29450.

Beyth, N. Houri-Haddad, Y. Domb, A. Khan, W. Hazan, R. Alternative Antimicrobial Approach, 2025.

Buzrul, S., 2015. Multi-pulsed high hydrostatic pressure treatment of foods. Foods 4, 173–183. https://doi.org/10.3390/foods4020173.

Cardoso, J.M.S., Galvão, A.M., Guerreiro, S.I., Leitão, J.H., Suarez, A.C., Carvalho, M.F.N.N., 2016. Antibacterial activity of silver camphorimine coordination polymers. Dalton Trans. 45, 7114.

Cardoso, J.M.S., Guerreiro, S.I., Lourenço, A., Alves, M.M., Montemor, M.F., Mira, N.P., 2017. Ag(I) Camphorimine complexes with antimicrobial activity towards clinically important bacteria and species of the *Candida* genus. PLoS One 12 (5), e0177355. https://doi.org/10.1371/journal.

Cardoso, J.M.S., Correia, I., Galvão, A.M., Marques, F., Carvalho, M.F.N.N., 2017. Synthesis of Ag(I) camphor sulphonylimine complexes and assessment of their cytotoxic properties against cisplatin-resistant A2780cisR andA2780 cell lines. J. Inorg. Biochem. 166, 55–63. https://doi.org/10.1016/j.jinorgbio.2016.11.003.

Carvalho, M.F.N.N., Leite, S., Costa, J.P., Galvão, A.M., Leitão, J.H., 2019. Ag(I) camphor complexes: antimicrobial activity by. J. Inorg. Biochem. 110791.

Chifiriuc, M.C., Filip, R., Constantin, M., Pircalabioru, G.G., Bleotu, C., Burlibasa, L., Ionica, E., Corcionivoschi, N., Mihaescu, G., 2022. Common themes in antimicrobial and anticancer drug resistance. Front. Microbiol. 13, 960693. https://doi.org/10.3389/fmicb.2022.960693.

Costa, J.P., Sousa, S.A., Galvão, A.M., Mata, J.M., Leitão, J.H., Carvalho, M.F.N.N., 2021. Key parameters on the antibacterial activity of silver camphor complexes. Antibiotics 10, 135.

Costa, J.P., Pinheiro, T., Martins, M.S., Carvalho 1, M.F.N.N., Feliciano, J.R., Leitão, J.H., Silva, R.A.L., Guerreiro, J.F., Alves, L.M.C., Custódio, I., Cruz, J., Marques, F., 2022. Biological activity of camphorimine complexes through metal selection. Antibiotics 11, 1010. https://doi.org/10.3390/antibiotics11081010.

Crisan, C.M., Mocan, T., Manolea, M., Lasca, L.I., Tabaran, F.-A., Mocan, L., 2021. Review on silver nanoparticles as a novel class of antibacterial solutions. Appl. Sci. 11, 1120. https://doi.org/10.3390/app11031120.

Dealey, C., Cameron, J., Arrowsmith, M., 2013. A study comparing two objective methods of quantifying the production of wound exudate. J. Wound Care 15 (4). https://doi.org/10.12968/jowc.2006.15.4.26897.

Dong, K., Li, Y., Luo, S., Zhang, F., Pan, H., Zhao, L., Wang, Y., Liao, X., 2021. Hydrostatic pressure boost rate and mode to enhance sterilization mediated by GroEL-interacting proteins. Food Control 126, 108091.

Evans, A., Kavanagh, K.A., 2021. Evaluation of metal-based antimicrobial compounds for the treatment of bacterial pathogens. J. Med. Microbiol. 70, 001363.

Ferguson, G.C., Martin, C.J., Rayner, C., 1991. Burn wound evaporation measurement of body fluid loss by probe evaporimeter and weight change. Clin. Phys. Physiol. Meas. 12 (2), 143–156. https://doi.org/10.1088/0143-0815/12/2/003.

Fontinha, D., Sousa, S.A., Morais, T.S., Prudêncio, M., Leitão, J.H., Le Gal, Y., Lorcy, D., Silva, R.A.L., Velho, M.F.G., Belo, D., Almeida, M., Guerreiro, J.F., Pinheiro, T., Marques Gold(III), F., 2020. bis(dithiolene) complexes: from molecular conductors to prospective anticancer, antimicrobial and antiplasmodial agents. Metallomics 24; 12 (6), 974–987. https://doi.org/10.1039/d0mt00064g.

Frei, A., Zuegg, J., Elliott, A.G., Baker, M., Braese, S., Brown, C., Chen, F., Dowson, C.G., Dujardin, G.N., Jung, A.P., King, A.P., Mansour, A.M., Massi, M., Moat, J., Mohamed, H.A., Renfrew, A.K., Rutldge, P.J., Sadler, P.J., Todd, M.H., Willans, C.E., Wilson, J.J., Cooper, M.A., Blaskovich, M.A.T., 2020a. Chem. Sci. 11, 2627–2639.

Frei, A., Zuegg, J., Elliott, A.G., Baker, M., Braese, S., Brown, C., Chen, F., Dowson, C.G., Dujardin, G., Jung, N., King, A.P., Mansour, A.M., Massi, M., Moat, J., Mohamed, H.A., Renfrew, A.K., Rutledge, P.J., Sadler, P.J., Todd, M.H., Willans, C.E., Wilson, J.J., Cooper, M.A., Blaskovich, M.A.T., 2020b. Metal complexes as a promising source for new antibiotics. Chem. Sci. 11, 2627–2639.

Garcia, L.V., Silva, D., Costa, M.M., Armés, H., Salema-Oom, M., Saramago, B., Serro, A. P., 2023. Antiseptic-loaded casein hydrogels for wound dressings. Pharmaceutics 15, 1–24. https://doi.org/10.3390/pharmaceutics15020334.

O. Grytsenko, P. Pukach, O. Suberlyak, N. Shakhovska, V. Karovič Jr, Usage of Mathematical Modeling and Optimization in Development of Hydrogel Medical Dressings Production.

O. Grytsenko, A. Pokhmurska, S. Suberliak, M. Kushnirchuk, M. Panas, V. Moravskyi, R. Kovalchuk, Technological features in obtaining highly effective hydrogel dressings for medical purposes, Eastern-Europ. J. Enterprise Technol., **2018**, *6*, 6(96). ISSN 1729-3774. DOI: 10.15587/1729-4061.2018.150690.

Harding, Keith & Carville, keryln & Chadwick, Paul & Moore, Zena & Nicodème, Marguerite & Percival, Steven L & Romanelli, Marco & Schultz, Gregory & Tariq, Gulnaz. **2019**. WUWHS Consensus Document: Wound Exudate, effective assessment and management.

https://reliefweb.int/report/world/antibacterial-agents-clinical-development-analysis-antibacterial-clinical-development. (accessed on 9 October **2023**).

https://www.who.int/news-room/fact-sheets/detail/antimicrobial-resistance (accessed 3 February 2023).

ISO 10993-4:2017 edition. Biological evaluation of medical devices Part 4: Selection of tests for interactions with blood. International Organization for Standardization, Geneva, Switzerland, **2017**. URL https://www.iso.org/standard/63448.html.

Jungwirth, U., Kowol, C.R., Keppler, B.K., Hartinger, C.G., Berger, W., Heffeter, P., 2011. Anticancer activity of metal complexes: involvement of redox processes. Antioxid. Redox Signal. 15 (4), 1085–1127. https://doi.org/10.1089/ars.2010.3663.

Junker, J.P., Kamel, R.A., Caterson, E.J., Eriksson, E., 2013. Clinical impact upon wound healing and inflammation in moist, wet, and dry environments. Adv. Wound Care (new Rochelle) 2 (7), 348–356. https://doi.org/10.1089/wound.2012.0412.

Klebowski, B., Depciuch, J., Parlińska-Wojtan, M., Baran, J., 2018. Applications of noble metal-based nanoparticles in medicine. Int. J. Mol. Sci. 19, 4031. https://doi.org/10.3390/ijms19124031.

Klode, J., Schöttler, L., Stoffels, I., Körber, A., Schadendorf, D., Dissemond, J., 2011. Investigation of adhesion of modern wound dressings: a comparative analysis of 56 different wound dressings. J. Eur. Acad. Dermatol. Venereol. 25, 933–939.

Lazarevi, T., Rilak, A., Bugar, Z.D., 2017. Platinum, palladium, gold and ruthenium complexes as anticancer agents: current clinical uses, cytotoxicity studies and future perspectives. Eur. J. Medicin. Chem. 142, 8–31. https://doi.org/10.1016/j.ejmech.2017.04.007.

Leitão, J.H., Sousa, S.A., Leite, S.A., Carvalho, M.F.N.N., 2018. Silver camphor imine complexes: novel antibacterial compounds from old medicines. Antibiotics 7, 65. https://doi.org/10.3390/antibiotics7030065.

Lewandowski, Ł., Bednarz-MisaKucharska, I., Kucharska, A.Z., Kubiak, A., Kasprzyk, P., Sozański, T., Przybylska, D., Piórecki, N., Krzystek-Korpacka, M., 2022. Cornelian cherry (*Cornus mas* L.) Extracts exert cytotoxicity in two selected melanoma cell lines-a factorial analysis of time-dependent alterations in values obtained with SRB and MTT assays. Molecules 27, 4193. https://doi.org/10.3390/molecules27134193.

P. Li, N. H. Kim, Siddaramaiah, J. H. ee Lee, Swelling behavior of polyacrylamide/laponite clay nanocomposite hydrogels: pH-sensitive property. Composites Part B: Engineering.

R. L. Lucaciu, A. C. Hangan, B. Sevastre, L. S. Oprean, Metallo-drugs in cancer therapy: past, present and future, molecules **2022**, *27*, 6485. Doi: 10.3390/molecules27196485.

Luo, J., Liu, W., Xie, Q., He, J., Jiang, L., 2023. Synthesis and characterisation of a novel poly(2-hydroxyethylmethacrylate)-chitosan hydrogels loaded cerium oxide nanocomposites dressing on cutaneous wound healing on nursing care of chronic wound. IET Nanobiotechnol. 17, 312–325. https://doi.org/10.1049/nbt2.12118.

Maver, T., Hribernik, S., Mohan, T., Smrke, D.M., Maver, U., Stana-Kleinschek, K., 2015. Functional wound dressing materials with highly tunable drug release properties. RSC Adv. 5, 77873. https://doi.org/10.1039/c5ra11972c.

Meakin, J.R., Hukins, D.W.L., Aspden, R.M., Imrie, C.T., 2003. Rheological properties of poly(2-hydroxyethyl methacrylate) (pHEMA) as a function of water content and deformation frequency. J. Mater. Sci. - Mater. Med. 14, 783–787. https://doi.org/10.1023/A:1025088405674.

Minsart, M., Van Vlierberghe, S., Dubruel, P., Mignon, A., 2022. Commercial wound dressings for the treatment of exuding wounds: an in-depth physico-chemical comparative study. Burns Trauma 10. https://doi.org/10.1093/burnst/tkac024.

Muhammad, N., Guo, Z., 2014. Metal-based anticancer chemotherapeutic agents. Curr. Opin. Chem. Biol. 19, 144–153. https://doi.org/10.1016/j.cbpa.2014.02.003.

Ndagi, U., Mhlongo, N., Soliman, M.E., 2017. Metal complexes in cancer therapy - an update from drug design perspective. Drug Des Devel Ther. 11, 599–616. https://doi.org/10.2147/DDDT.S119488. PMID: 28424538; PMCID: PMC5344412.

Nguyen, N., Dulai, A.S., Adnan, S., Khan, Z.E., Sivamani, R.K., 2025. Narrative review of the use of hydrocolloids in dermatology: applications and benefits. J. Clin. Med. 14 (4), 1345. https://doi.org/10.3390/jcm14041345. PMID: 40004874; PMCID: PMC11856799.

Otaka, A., Yamamoto, T., Yamaoka, T., 2024. High pressure pasteurization: simultaneous native tissue decellularization and sterilization. Regenerat. Therapy 26, 2–8. https://doi.org/10.1016/j.reth.2024.01.012.

Paradiso, P., Chu, V., Santos, L., Serro, A.P., Colaço, R., Saramago, B., 2015. Effect of plasma treatment on the performance of two drug-loaded hydrogel formulations for therapeutic contact lenses. J. Biomed. Mater. Res. Part B 103B, 1059–1068.

Pires, T., Oliveira, A.S., Marques, A.C., Salema-Oom, M., Figueiredo-Pina, C.G., Silva, D., Serro, A.P., 2022. Effects of non-conventional sterilisation methods on PBO-reinforced PVA hydrogels for cartilage replacement. Gels 8, 640. https://doi.org/10.3390/gels8100640.

Radhakumary, C., Nandkumar, A.M., Nair, P.D., 2011. Hyaluronic acid-g-poly(HEMA) copolymer with potential implications for lung tissue engineering. Carbohydr. Polym. 85, 439–445.

Rafique, S., Idrees, M., Nasim, A., Akbar, H., Athar, A., 2010. Transition metal complexes as potential therapeutic agents. Biotechnol. and Molec. Biol. Rev. 5 (2), 38–45. http://www.academicjournals.org/BMBR.

Rahmani, H., Najaki, S.H.M., Ashori, A., Fashapoyeh, M.A., Moheseni, F.A., Torkaman, S., 2020. Preparation of chitosan-based composites with urethane cross linkage and evaluation of their properties for using as wound healing dressing. Carbohydr. Polym. 230, 115606. https://doi.org/10.1016/j.carbpol.2019.115606.

Rainho, P., Salema-Oom, M., Pinto, C.A., Saraiva, J.A., Saramago, B., Silva, D.C., Serro, A.P., 2025. Polyvinyl alcohol/casein hydrogels with oxymatrine eluting ability for cancer-related wound management. Biomater. Sci. 13, 2755–2766. https://doi.org/10.1039/d5bm00191a.

Ritger, P., Peppas, N., 1987. A simple equation for description of solute release I. Fickian and non-fickian release from non-swellable devices in the form of slabs, spheres, cylinders or discs. J. Control. Release 5, 23–26.

Schreml, S., Szeimies, R.M., Prantl, L., Karrer, S., Landthaler, M., Babilas, P., 2010. Br. J. Dermatol, Oxygen Acute Chronic Wound Heal. 163 (2), 257–268. https://doi.org/10.1111/j.1365-2133.2010.09804.x.

Shariq, A., Rasheed, Z., Alghsham, R.S., Abdulmonem, W.A., 2023. Candida auris: an emerging fungus that presents a serious global health threat. Int. J. Health Sci. (qassim) 17 (2), 1–2. PMID: 36891046.

Sharma, B., Shukla, S., Rattan, R., Fatima, M., Goel, M., Bhat, M., Dutta, S., Ranjan, R.K., Sharma, M., 2022. Antimicrobial agents based on metal complexes: present situation and future prospects. Int. J. Biomater. 8, 6819080. https://doi.org/10.1155/2022/6819080. PMID: 36531969; PMCID: PMC9754840.

Singh, B., Dhimanm, A., 2015. Designing bio-mimetic moxifloxacin loaded hydrogel wound dressing to improve antioxidant and pharmacology properties. RSC Adv. 5 (55), 44666–44678. https://doi.org/10.1039/C5RA06857F.

Singh, B., Sharma, S., Dhiman, A., 2013. Design of antibiotic containing hydrogel wound dressings: biomedical properties and histological study of wound healing. Int. J. Pharm. 457, 82–91. https://doi.org/10.1016/j.ijpharm.2013.09.028.

Slack, S. M. Properties of biological fluids. In Biomaterials Science: An Introduction to Materials in Medicine, In: 4th ed.: Wagner, W.R., Sakiyama-Elbert, S.E., Zhang, G., Yaszemski, M.J., Eds.; Academic Press: London, UK, **2020**, 1519–1524. ISBN 978-0-12-816137-1.

Tang, Q., Yu, J.-R., Chen, L., Zhu, J., Hu, Z.-M., 2010. Preparation and properties of morphology controlled poly(2-hydroxyethyl methacrylate)/poly(N-vinyl pyrrolidone) double networks for biomedical use. Curr. Appl Phys. 10, 766–770. https://doi.org/10.1016/j.cap.2009.09.012.

Teixeira, J., Lumack do Monte, Z., Tenreiro, S., Salema-Oom, M., Silva, D.C., Saramago, B., Serro, A.P., 2024. Citicoline eluting hydrogels for therapeutic contact lenses intended to treat neurodegenerative diabetic ocular diseases. Inter. J. Pharmaceutics 667, 124908. https://doi.org/10.1016/j.ijpharm.2024.124908.

Terreni, M., Taccani, M., Pregnolato, M., 2021. New antibiotics for multidrug-resistant bacterial strains: latest research developments and future perspectives. Molecules 26, 2671. https://doi.org/10.3390/molecules26092671.

Thomas, S., Fear, M., Humphreys, J., Disley, L., Waring, M., 1996. The effect of dressings on the production of exudate from venous leg ulcers. Wounds: Compendium Clin. Res. Prac. 8 (5), 145–150.

Topete, A., Pinto, C.A., Barroso, H., Saraiva, J.A., Barahona, I., Saramago, B., Serro, A.P., 2020. High hydrostatic pressure as sterilization method for drug-loaded intraocular lenses. ACS Biomater Sci. Eng. 6 (7), 4051–4061.

Tran, Q.H., Nguyen, V.Q., Le, A.-T., 2013. Silver nanoparticles: synthesis, properties, toxicology, applications and perspectives. Adv. Nat. Sci. Nanosci. Nanotechnol. 4, 033001. https://doi.org/10.1088/2043-6262/4/3/033001.